

Gold(I)-Catalyzed Dynamic Kinetic Enantioselective Intramolecular Hydroamination of Allenes

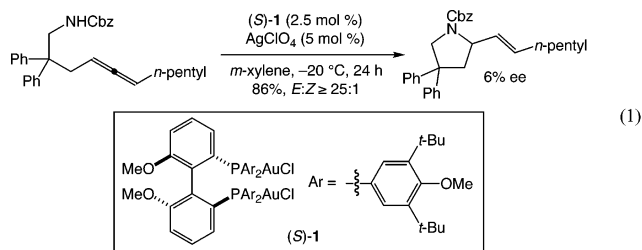
Zhibin Zhang, Christopher F. Bender, and Ross A. Widenhoefer*

French Family Science Center, Duke University, Durham, North Carolina 27708–0346

Received August 12, 2007; E-mail: rwidenho@chem.duke.edu

Dynamic kinetic asymmetric transformations (DYKATs) constitute a powerful class of reactions with the potential to convert both enantiomers of a racemic starting material into a single enantiomerically pure product with concomitant increase in molecular complexity.¹ Although numerous DYKATs have been reported,¹ few form a C–X (X = C, N, O) bond at a stereogenic center, and absent are DYKATs that involve addition across a C=C bond.² Because a number of transition metals catalyze the functionalization³ and/or racemization^{4,5} of allenenes, axially chiral allenenes represent attractive substrates for the development of DYKATs that involve both C–X bond formation and C=C bond functionalization. Nevertheless, DYKATs that employ axially chiral allenenes as substrates remain exceedingly rare.^{6,7}

We recently reported the Au(I)-catalyzed enantioselective intramolecular hydroamination of *N*-(γ -allenyl) carbamates catalyzed by mixtures of [(*S*)-3,5-*t*-Bu-4-MeO-MeOBIPHEP]Au₂Cl₂ [(*S*)-**1**] and AgClO₄.^{8,9} Although cationic Au(I) complexes racemize allenenes,⁵ hydroamination of *N*-(γ -allenyl) carbamates that contained a 1,3-disubstituted allenyl moiety catalyzed by (*S*)-**1**/AgClO₄ occurred with high diastereoselectivity/low enantioselectivity in a substrate-controlled process (eq 1).⁸ We reasoned that employment of trisubstituted allenenes might both attenuate substrate stereocontrol and retard the rate of C–N bond formation relative to racemization, leading to dynamic kinetic enantioselective hydroamination (DKEH). Indeed, here we report the gold(I)-catalyzed DKEH of *N*-(γ -allenyl) carbamates that possess trisubstituted allenyl groups.



Treatment of a number of *N*-(γ -allenyl) carbamates that possessed an axially chiral trisubstituted allenyl group with a catalytic mixture of (*S*)-**1**/AgClO₄ led to predominant formation of one of four possible 2-vinyl pyrrolidine stereoisomers (Table 1). For example, reaction of benzyl 6-methyl-1,2,2-diphenyl-4,5-octadienyl carbamate (**2a**) with a catalytic 1:2 mixture of (*S*)-**1** (2.5 mol %) and AgClO₄ (5 mol %) in *m*-xylene at room temperature for 24 h led to isolation of a 49:14:1.9:1 mixture of (*R,Z*)-**3a**/*(R,E)*-**3a**/*(S,E)*-**3a**/*(S,Z)*-**3a** in 94% combined yield (Table 1, entry 1).^{10,11} The formation of (*R,Z*)-**3a** as 74% of the reaction mixture pointed to the dynamic nature of enantioselective hydroamination. Accordingly, when the reaction of **2a** with (*S*)-**1**/AgClO₄ was monitored periodically by HPLC equipped with chiral stationary phase, the resulting concentration versus time plot revealed that the relative concentration of (*R*)-**2a** fell below that of (*S*)-**2a** within the first 6% conversion [(*R*)-**2a**/

Table 1. Dynamic Kinetic Enantioselective Hydroamination (DKEH) of *N*-(γ -Allenyl) Carbamates Catalyzed by a Mixture of (*S*)-**1** (2.5 mol %) and AgClO₄ (5 mol %) in *m*-Xylene at 23 °C

entry	allene	yield (<i>Z</i>)- 3 + (<i>E</i>)- 3 (%) ^a	(<i>Z</i>)- 3 / (<i>E</i>)- 3	ee (<i>Z</i>)- 3 (%)	ee (<i>E</i>)- 3 (%)
1	2a (X = CPh ₂ , R ¹ = Me, R ² = Et)	94	3.1:1	96	76
2	2b (X = CPh ₂ , R ¹ = Me, R ² = <i>n</i> -hexyl)	99	10.1:1	91	9
3 ^b	2c (X = CPh ₂ , R ¹ = Me, R ² = <i>i</i> -Bu)	99	2.6:1	87	54
4	2d (X = CPh ₂ , R ¹ = Me, R ² = <i>i</i> -Pr)	94	2.0:1	95	67
5 ^c	2e (X = CPh ₂ , R ¹ = Me, R ² = <i>t</i> -Bu)	52	≤ 1:25	2	—
6	2f (X = CPh ₂ , R ¹ = Et, R ² = <i>n</i> -hexyl)	86	4.3:1	84	47
7	2g (X = CH ₂ , R ¹ = Me, R ² = <i>n</i> -hexyl)	87	2.4:1	75	45

^a Yield of isolated material of >95% purity. ^b Reaction run at 0 °C for 24 h followed by 23 °C for 24 h. ^c Reaction run at 60 °C for 212 h followed by 100 °C for 48 h.

(*S*)-**2a** = 45.8:48.1; 2.4% ee] and remained deficient throughout 95% conversion (Figure 1).^{10,11} This behavior is indicative of a dynamic kinetic process in which (*R*)-**2a** (matched) is converted to product more rapidly than is (*S*)-**2a** (mismatched) and is continually replenished via racemization.

Mass balance requires formation of (*R,Z*)-**3a** from (*R*)-**2a** in the matched reaction manifold in the reaction of **2a** with (*S*)-**1**/AgClO₄. To determine whether (*R,E*)-**3a** was formed in the matched or mismatched reaction manifold, we analyzed the (*R,Z*)-**3a**/*(R,E)*-**3a** ratio as a function of conversion. If both (*R,Z*)-**3a** and (*R,E*)-**3a** were formed in the matched reaction manifold, the (*R,Z*)-**3a**/*(R,E)*-**3a** ratio should remain constant with increasing conversion. Conversely, if (*R,Z*)-**3a** and (*R,E*)-**3a** were formed in matched and mismatched reaction manifolds, respectively, the (*R,Z*)-**3a**/*(R,E)*-**3a** ratio should decrease from its initial value due to deviation from true Curtin–Hammett conditions.¹² In support of this latter scenario, the (*R,Z*)-**3a**/*(R,E)*-**3a** ratio decreased from an initial value of 3.8 to 3.5 at complete conversion (Figure 1).

Analysis of concentration versus time plots for the hydroamination of enantiomerically enriched (*R*)-**2a** (44% ee) catalyzed by either (*S*)-**1**/AgClO₄ (matched) or (*R*)-**1**/AgClO₄ (mismatched) confirmed rapid racemization of **2a** under the reaction conditions (Figure 1).¹¹ Furthermore, these experiments supported our assignment of the major products formed in the matched and mismatched reaction manifolds in the DKEH of **2a**. In the case in which the

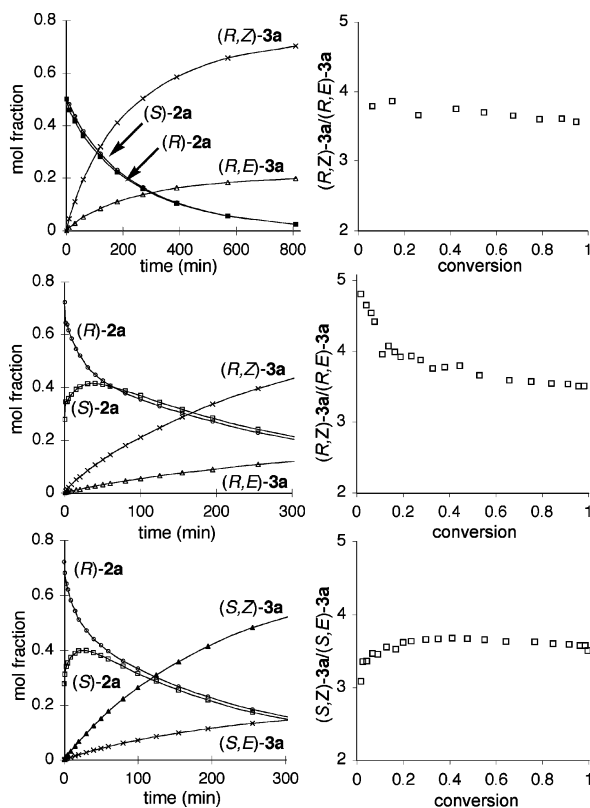
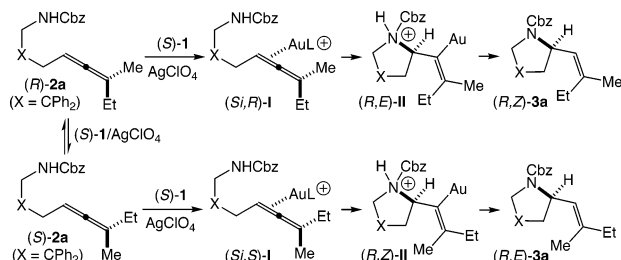


Figure 1. Plots of concentration versus time (left-hand column, minor enantiomers omitted for clarity) and *Z/E* ratio versus conversion (right-hand column) for the cyclization of *rac*-**2a** catalyzed by (*S*)-**1**/AgClO₄ (top plots), a ~3:1 mixture of (*R*)-**2a** and (*S*)-**2a** catalyzed by (*S*)-**1**/AgClO₄ (middle plots), and a ~3:1 mixture of (*R*)-**2a** and (*S*)-**2a** catalyzed by (*R*)-**1**/AgClO₄ (bottom plots) in *m*-xylene at 23 °C. Catalyst loading: **1** = 2.5 mol %; AgClO₄ = 5 mol %.

Scheme 1



matched enantiomer was initially present in excess [(*R*)-**2a**/(*S*)-**1**], the (*R,Z*)-**3a**/(*R,E*)-**3a** ratio decreased rapidly from 4.5 to 3.9 early in the reaction (0–20% conversion), whereas in the reaction in which the mismatched enantiomer was initially present in excess [(*R*)-**2a**/(*R*)-**1**], the (*S,Z*)-**3a**/(*S,E*)-**3a** ratio increased from 3.1 to 3.6 early in the reaction (0–20% conversion) (Figure 1). In both cases, the product ratio mirrored the rapidly changing (*R*)-**2a**/(*S*)-**2a** ratio early in the reaction.

The experiments described above support the mechanism for the DKEH of *rac*-**2a** catalyzed by (*S*)-**1**/AgClO₄ depicted in Scheme 1. In the major pathway of the matched reaction manifold, complexation of gold to the *Si* face of the internal C=C bond of (*R*)-**2a** followed by outer-sphere cyclization of gold–allene complex (*Si,R*)-**I** would form alkenyl gold σ -complex (*R,E*)-**II** (Scheme 1). Deprotonation of (*R,E*)-**II** followed by protonolysis of the Au–C

bond with retention of configuration¹³ would form (*R,Z*)-**3a**. In the major pathway of the mismatched reaction manifold, outer-sphere cyclization of gold–allene complex (*Si,S*)-**I** followed by deprotonation/protonolysis would form (*R,E*)-**3a**. Analogous outer-sphere pathways have been proposed on the basis of stereochemical analysis for the gold(I)-catalyzed addition of nucleophiles to C–C multiple bonds.¹⁴ Although the mechanism of racemization remains unclear,⁵ the formation of (*R,Z*)-**3a** and (*R,E*)-**3a** in discrete reaction manifolds argues strongly against racemization of **2a** in the C–N bond forming manifold.

In summary, we have presented the first examples of the dynamic kinetic enantioselective hydroamination (DKEH) of axially chiral allenes, and we provide experimental evidence for the dynamic nature and mechanism of these transformations.

Acknowledgment. Acknowledgment is made to the NSF (CHE-0555425), NIH (GM-080422), and Johnson&Johnson for support of this research. We thank Dr. David Pham for determining the X-ray crystal structure of (*R,S*)-**S13**.

Supporting Information Available: Experimental procedures, spectroscopic data, and scans of NMR spectra and HPLC traces (PDF). This material is available free of charge via the Internet at <http://pubs.acs.org>.

References

- (a) Vedejs, E.; Jure, M. *Angew. Chem., Int. Ed.* **2005**, *44*, 3974. (b) Pellissier, H. *Tetrahedron* **2003**, *59*, 8291. (c) Pamies, O.; Bäckvall, J.-E. *Chem. Rev.* **2003**, *103*, 3247.
- (a) Hayashi, T.; Konishi, M.; Fukushima, M.; Mise, T.; Kagotani, M.; Tajika, M.; Kumada, M. *J. Am. Chem. Soc.* **1982**, *104*, 180. (b) Hayashi, T.; Yamamoto, A.; Hojo, M.; Ito, Y. *J. Chem. Soc., Chem. Commun.* **1989**, 495. (c) Trost, B. M.; Toste, F. D. *J. Am. Chem. Soc.* **1999**, *121*, 3543. (d) Trost, B. M.; Patterson, D. E.; Hembre, E. J. *J. Am. Chem. Soc.* **1999**, *121*, 10834. (e) Cook, G. R.; Shanker, P. S.; Pararajasingham, K. *Angew. Chem., Int. Ed.* **1999**, *38*, 110. (f) Braun, M.; Kotter, W. *Angew. Chem., Int. Ed.* **2004**, *43*, 514. (g) Xu, K.; Lalic, G.; Sheehan, S. M.; Shair, M. D. *Angew. Chem., Int. Ed.* **2005**, *44*, 2259.
- (a) Ma, S. *Chem. Rev.* **2005**, *105*, 2829. (b) *Modern Allene Chemistry*; Krause, N.; Hashmi, A. S. K., Eds.; Wiley-VCH: Weinheim, Germany, 2004. (c) Bates, R. W.; Satcharoen, V. *Chem. Soc. Rev.* **2002**, *31*, 12.
- (a) Horvath, A.; Bäckvall, J.-E. *Chem. Commun.* **2004**, 964. (b) Ogoshi, S.; Nishida, T.; Shinagawa, T.; Kurosawa, H. *J. Am. Chem. Soc.* **2001**, *123*, 7164. (c) Claesson, A.; Olsson, L.-I. *J. Chem. Soc., Chem. Commun.* **1979**, 524.
- Sherry, B. D.; Toste, F. D. *J. Am. Chem. Soc.* **2004**, *126*, 15978.
- (a) Trost, B. M.; Fandrick, D. R.; Dinh, D. C. *J. Am. Chem. Soc.* **2005**, *127*, 14186. (b) Imada, Y.; Ueno, K.; Kutsuwa, K.; Murahashi, S.-I. *Chem. Lett.* **2002**, 140. (c) Mikami, K.; Yoshida, A. *Angew. Chem., Int. Ed. Engl.* **1997**, *36*, 858.
- For the kinetic resolution of allenes, see: (a) Sweeney, Z. K.; Salsman, J. L.; Andersen, R. A.; Bergman, R. G. *Angew. Chem., Int. Ed.* **2000**, *39*, 2339. (b) Noguchi, Y.; Takiyama, H.; Katsuki, T. *Synlett* **1998**, 543.
- Zhang, Z.; Bender, C. F.; Widenhoefer, R. A. *Org. Lett.* **2007**, *9*, 2887.
- See also: LaLonde, R. L.; Sherry, B. D.; Kang, E. J.; Toste, F. D. *J. Am. Chem. Soc.* **2007**, *129*, 2452.
- Control experiments ruled out both the isomerization of (*E*)-**3a** and (*Z*)-**3a** under reaction conditions and the contribution of AgClO₄- or HClO₄-catalyzed processes to the racemization or enantioselective hydroamination of **2a**. Mixtures of HOTf and P–P, AgOTf and P–P, or Pt(P–P)Cl₂ and AgOTf [P–P = (*S*)-3,5-*t*-Bu-4-MeO-MeOBIPHEP] were also ineffective catalyst systems for the DKEH of **2a** (see Supporting Information).
- See Supporting Information for the assignment of absolute configuration of (*R,Z*)-**3a** and (*R,E*)-**3a** and for the synthesis of enantiomerically enriched (*R*)-**2a**.
- (a) Kitamura, M.; Tokunaga, M.; Noyori, R. *Tetrahedron* **1993**, *49*, 1853. (b) Andraos, J. *J. Phys. Chem. A* **2003**, *107*, 2374. (c) Kitamura, M.; Tokunaga, M.; Noyori, R. *J. Am. Chem. Soc.* **1993**, *115*, 144.
- Johnson, A.; Puddephatt, R. J. *J. Chem. Soc., Dalton Trans.* **1978**, 980.
- (a) Kennedy-Smith, J. J.; Staben, S. T.; Toste, F. D. *J. Am. Chem. Soc.* **2004**, *126*, 4526. (b) Zhang, J.; Yang, C.-G.; He, C. *J. Am. Chem. Soc.* **2006**, *128*, 1798. (c) Zhang, Z.; Liu, C.; Kinder, R. E.; Han, X.; Qian, H.; Widenhoefer, R. A. *J. Am. Chem. Soc.* **2006**, *128*, 9066. (d) Hashmi, A. S. K.; Weyrauch, J. P.; Frey, W.; Bats, J. W. *Org. Lett.* **2004**, *6*, 4391. (e) Liu, Y.; Song, F.; Song, Z.; Liu, M.; Yan, B. *Org. Lett.* **2005**, *7*, 5409. (f) Zhang, Z.; Widenhoefer, R. A. *Angew. Chem., Int. Ed.* **2007**, *46*, 283.

JA0760731